

Research

# *Accurate Measurement, Using Natural Sunlight, of Silicon Solar Cells*

William M. Keogh<sup>\*†</sup> and Andrew W. Blakers

*Centre for Sustainable Energy Systems, The Australian National University, Canberra, 0200, Australia*

*The light source is very important when measuring solar cells. Commonly used light sources—good-quality solar simulators—are expensive and have far from ideal characteristics. Computer modelling described in this work strongly suggests that testing of silicon solar cells under natural sunlight is simpler, cheaper, and more accurate than all but the most careful simulator measurements. Direct-beam solar spectra were generated with the model SMARTS2 for a range of atmospheric conditions, and a broad range of silicon cells (efficiencies 6–25%) were then simulated under these spectra. These simulations showed that measurement uncertainty of less than 5% should be achievable. Climate data for locations within 45° of the equator show that the required atmospheric conditions should occur commonly in summer. Finally, it is shown that the important atmospheric conditions can be measured without expensive equipment. Copyright © 2004 John Wiley & Sons, Ltd.*

KEY WORDS: characterisation; modelling; SMARTS2; natural sunlight

## INTRODUCTION

Accurate measurement of solar cells is essential, both to improve technologies and to predict performance in operation. This work concentrates on the problem of accurate measurement of small numbers of cells for use as references or to set efficiency records.

The most expensive part of a solar cell measurement set-up, and also the major source of error, is the light source. The major problems that can occur due to the light source are: that the light intensity is incorrect; that the spectrum does not match the relevant standard spectrum (spectral mismatch); that the light intensity varies over the illuminated area (nonuniformity); that light can be reflected around the test fixture unpredictably (multiple reflections); and that the light intensity changes over time (instability).

All solar simulators have substantial non-idealities. If a reference cell is used that is similar to the test cells and has been accurately calibrated previously, the errors due to the non-idealities will be largely cancelled. This is the basis on which the vast majority of routine cell measurements are made. The alternative, in the absence of a matched reference cell, is to correct for the non-idealities. This is the approach taken by standards laboratories. Spectral mismatch errors are the hardest to eliminate. They are corrected by the technique of spectral

<sup>\*</sup>Correspondence to: William M. Keogh, Centre for Sustainable Energy Systems, The Australian National University, Canberra, 0200, Australia.

<sup>†</sup>E-mail: William.Keogh@ieee.org

Contract/grant sponsor: ERDC.

mismatch correction.<sup>1,2</sup> This requires accurate measurement of the spectral irradiance of the light source, and the spectral responses of both the test and reference cells. It is a complex and expensive procedure, so is rarely used outside of standards laboratories.

Natural sunlight is, in many respects, far superior to a solar simulator for accurate measurement of solar cells. Under the right atmospheric conditions its spectrum is, unsurprisingly, an excellent match to the standard spectra.<sup>3</sup> This eliminates the need for a reference cell with a spectral response matched to the test cell. Sunlight has superb uniformity over any area, which eliminates the need for a reference cell of the same size. Sunlight is also extremely well collimated, making it easy to eliminate multiple reflections. Finally, the stability of natural sunlight, though not particularly good, is not important as the excellent uniformity allows the reference and test cells to be measured simultaneously, side-by-side.

The limited availability of sunlight is not a major disadvantage to groups whose main business is making solar cells. Most of the cells will be produced according to a standard recipe, so will have similar characteristics. Cell recipes evolve slowly, so new reference cells will not need to be created often. Waiting for good weather is therefore not likely to be a major problem.

The superiority of natural sunlight as a light source has been recognised previously. Many primary calibration techniques, past and present, use it. In the early days of solar cell calibration the NASA–Lewis method<sup>4,5</sup> used direct-beam natural sunlight without spectral mismatch correction. In the present day, NREL's primary-standard calibration method also uses direct-beam sunlight, though now with spectral mismatch correction.<sup>6–8</sup> There are also two ASTM methods that use natural sunlight: E1039<sup>9</sup> and E1125.<sup>7</sup> However, none of these methods are applicable for convenient, low-cost measurements. They all require expensive, specialised equipment, and some are quite complex. To get very high measurement accuracy they also tend to specify hard limits on atmospheric conditions. In contrast, the method described in this work does not require expensive equipment, and is relatively convenient. It also shows the variation of measurement accuracy with atmospheric conditions, allowing users to decide if conditions are good enough for their purposes.

This work considers measurement with respect to both AM1.5G and AM1.5D standard spectra. For AM1.5G measurements, it might seem sensible to measure under global illumination. However, consideration of the potential error sources shows that it is preferable to measure under direct-beam illumination. Conveniently, typical AM1-direct spectra are very similar to the AM1.5G standard, so direct-beam sunlight can be used to 'simulate' the global spectrum with high accuracy. The most important factor in favour of direct-beam measurement is the accuracy of the reference device—pyrheliometers (direct-beam) are more accurate than pyranometers (global). Typically, ~2% compared with ~5%.<sup>10</sup> Secondly, measurement under global illumination may allow local reflections to illuminate the test cell and reference cell differently. Thirdly, standards laboratories mostly use well-collimated solar simulators. Since the main purpose of measurement for a cell manufacturer is to get measurements that are consistent with the standards laboratories, and since cell performance may be slightly different under wide-angle and collimated illumination, it is preferable to use a well-collimated light source. Finally, part of the global spectrum is light that is multiply reflected between sky and land. The land-cover characteristics, which are variable and hard to measure, will therefore influence measurements under global illumination. All of these factors weigh in favour of the use of direct-beam natural sunlight for accurate measurements. Consequently, this work considers only measurements under direct-beam illumination.

Standards laboratories use the best available measurement techniques, and it is useful to review the accuracy of these techniques as a benchmark against which simpler techniques can be compared. The accuracies of the best techniques have been studied in two major ways: theoretical analyses predicting the total measurement uncertainty, and inter-laboratory comparisons where cells were circulated amongst different laboratories to determine the reproducibility of real measurements. Theoretical analyses<sup>6,11</sup> have found that NREL's primary calibration technique should have an uncertainty of 0.7–1% (*all uncertainties referred to in this paper are 2 standard deviations*), and their secondary standard simulator technique should have an uncertainty of 1.1%. Inter-laboratory comparisons however, have generally shown reproducibilities substantially worse than the theoretical analyses predict. For the restricted case of  $2 \times 2$  cm high-quality silicon cells measured by a select group of laboratories,  $I_{sc}$  reproducibility of about 2% can be achieved. This is documented in the PEP93<sup>12</sup> (1993–95) and PEP87<sup>13</sup> (1987–89) intercomparisons. For the more general case of large-area cells and/or unusual spectral responses, the intercomparison results have not been as good. A second part of PEP93, testing a

variety of cells, found the reproducibility of maximum power measurement to be 6% for large-area ( $10 \times 10$  cm) silicon cells (the reproducibility for  $I_{sc}$  was not reported, but is presumably a bit smaller than 6%). ASTM also conducted a comparison between seven laboratories during 1992–94 for its secondary reference calibration method, E1362,<sup>14</sup> and found  $I_{sc}$  reproducibility to be 5.7% (cell types and sizes not reported). Finally, an informal intercomparison between four laboratories (Sandia, NREL, F-ISE & JQA)<sup>15</sup> found a reproducibility of 1.5% for two very similar high-quality silicon cells of  $\sim 7 \times 7$  cm. It appears that 2% reproducibility may sometimes be achieved for larger cells, but not always. There is also the question of how routine measurements compare to the results reported above. The intercomparisons have not been performed blind, so the laboratories probably took special care with these particular measurements, and routine measurements may not be quite as good. To summarise all of these studies, measurement uncertainty under the best possible conditions may be as low as 2%, but the uncertainty in routine measurements is probably in the range 2–5%.

The review of measurement techniques described above showed that natural sunlight is an excellent light source, but existing techniques using it are expensive and difficult. This led to some questions. Could a convenient, simple, and low cost natural sunlight calibration procedure be developed? How accurate would it be under a typical range of atmospheric conditions? What are the important atmospheric conditions? Could they be measured without specialised equipment? And how common are good conditions?

These questions were addressed in this work by computer modelling. Solar spectra were simulated with the model SMARTS2 for a range of low-air-mass, clear-sky conditions. The spectra of a few artificial light sources (solar simulators) were included too, for comparison. A large group of solar cells were then simulated under the different spectra. The cells were chosen to be representative of almost any crystalline silicon cell likely to be made (efficiencies 6–25%). Over a million cell/spectrum combinations were tried. The spectral mismatch error was then calculated for each cell/spectrum combination. From this dataset, the worst-case spectral mismatch error was extracted for each spectrum. The result is a group of plots of worst-case spectral mismatch error as a function of the important atmospheric conditions—air-mass, turbidity, and precipitable water. This work also presents the results of some preliminary experiments to verify the modelling.

The sensitivity to changes in atmospheric conditions of silicon cell measurement with respect to a thermal detector has been well studied in the past. Examples include the development of the NASA–Lewis calibration method,<sup>4</sup> and work by Mueller<sup>16</sup> and Osterwald.<sup>17</sup> All previous work has, however, treated only a small number of high-quality cells. As spectral mismatch is worse for poor-quality cells, this previous work tends to underestimate the spectral mismatch error. As an example, Osterwald found that for poor conditions,  $AM = 2$ ,  $\beta = 0.1$ ,  $w = 1$  cm, the spectral mismatch error was  $-2\%$  (only one cell studied). This work shows, for the same conditions, a range of spectral mismatch errors from  $-10\%$  to  $+5\%$ .

The principle of this work—that natural sunlight is a much better light source than any low-cost simulator—should apply to other PV technologies. However, this cannot be said for certain until the calculations have been done for other technologies. The mismatch-error estimates calculated in this work are specific to crystalline silicon and so cannot be directly applied to other technologies.

This paper is a condensed version of part of the first author's PhD Thesis.<sup>18</sup> The full version is available online.

## SOLAR SPECTRUM MODELLING WITH SMARTS2

### Introduction

The spectrum of natural sunlight was modelled in this work using the code SMARTS2 (V2.8).<sup>19,20</sup> It is a parametric model, so is relatively simple to use, but it is almost as accurate as rigorous codes such as MODTRAN.<sup>21</sup> The suitability of SMARTS2 for this purpose is supported by NREL and ASME having recently chosen it for the generation of revised AM1.5G and AM1.5D standard spectra.<sup>22</sup>

The direct-beam sunlight spectrum in SMARTS2 depends on roughly a dozen atmospheric parameters. As a first step in the simulations, a sensitivity analysis was conducted to determine which of these parameters were important. This analysis showed that only five parameters—air-mass, precipitable water, turbidity, altitude, and

Table I. Atmospheric parameter values used in detailed simulation

| Atmospheric parameter         | Values                       |
|-------------------------------|------------------------------|
| Air mass, AM                  | 1.0, 1.2, 1.4, 1.6, 1.8, 2.0 |
| Turbidity, $\beta$            | 0.00, 0.02, 0.05, 0.1, 0.2   |
| Precipitable water, $w$       | 0.5, 1, 2, 3, 5 atm cm       |
| NO <sub>2</sub>               | 0.1, 1, 5 matm cm            |
| Altitude                      | 0, 1, 2 km                   |
| Ozone                         | 0.34 atm cm                  |
| Season                        | Summer                       |
| Latitude                      | 40°                          |
| Daily average air temperature | 20°                          |
| Ambient air temperature       | 25°                          |
| Aerosol model                 | Shettle and Fenn, rural      |

NO<sub>2</sub>—have a significant influence on spectral mismatch. This was true for both AM1.5G and AM1.5D standard spectra. Three of these parameters—air-mass, turbidity, and precipitable water—have a major influence. These parameters were varied in the simulations over their naturally occurring ranges, and are measured as part of the calibration technique described in this paper. The other two parameters, NO<sub>2</sub> and altitude, are less important, and so were switched between extreme values in the simulations. There is no need to measure them in practice—the new method includes the worst-case effect of their variation. The remaining parameters, such as ozone (despite its high public profile, ozone actually has little effect on solar cell measurement, as there are not many ultraviolet photons in the solar spectrum), temperature and season have minimal effect, so were set to typical values in the simulation. The atmospheric parameter values used for the detailed simulations are shown in Table I.

The results of this work also contain results for three solar simulators, which were determined using typical spectra published for each simulator and fed into the simulations exactly the same as the natural sunlight spectra. The simulators used were an ELH projector lamp<sup>23</sup> (commonly used for very cheap solar simulators), an Oriel 1 kW solar simulator with AM1.5G filter<sup>24</sup> (a typical commercial solar simulator, ~US\$20 000), and a Spectrolab X-25<sup>23</sup> (one of the best solar simulators available, ~US\$200 000). The comparison could be made only for the case of a silicon reference cell as the published spectra did not extend past 1.1  $\mu\text{m}$ .

Descriptions of the 3 crucial atmospheric parameters—air-mass, precipitable water, and turbidity—follow. Low-cost techniques to measure them are described as well.

#### *Air-mass*

Air-mass (AM) is a measure of the optical path-length through the atmosphere. For the low-air-mass conditions of interest in this work, it is given by  $\text{AM} = \sec(Z)$ , where  $Z$  is the zenith angle (when the sun is directly overhead  $Z = 0^\circ$ ). The zenith angle can be calculated from the latitude, longitude, date, and time. Suitable codes are available in SMARTS2,<sup>20</sup> SPECTRL2,<sup>25</sup> and in Michalsky.<sup>26</sup>

SMARTS2 does not use a pressure-corrected (and hence altitude-corrected) air-mass. The corrections are made via separate inputs for altitude and air pressure. Consequently, in this work the air-mass referred to is not pressure corrected.

#### *Precipitable water*

Precipitable water  $w$  is the total amount of water in a vertical column of the atmosphere. It is usually specified in terms of centimetres of liquid water (atm cm). Water causes heavy absorption in bands in the IR beyond 900 nm, effectively making the spectrum bluer. In temperate locations,  $w$  is usually in the range 1–3 cm. In tropical locations,  $w$  may be as high as 5 cm. In deserts or below freezing conditions,  $w$  may be as low as 0.5 cm.

Accurate measurement of precipitable water requires radiosonde balloon soundings, but it is possible to estimate precipitable water with sufficient accuracy using only ground-level relative humidity and temperature. Precipitable water is given by Equation (1), derived from two works by Gueymard.<sup>27,28</sup>

$$w = 0.1 \left( 0.4976 + 1.5265 \frac{T}{273.15} + \exp \left[ 13.6897 \frac{T}{273.15} - 14.9188 \left( \frac{T}{273.15} \right)^3 \right] \right) \times \left( 216.7 \frac{R_H}{100T} \exp \left[ 22.330 - 49.140 \frac{100}{T} - 10.922 \left( \frac{100}{T} \right)^2 - 0.39015 \frac{T}{100} \right] \right) \quad (1)$$

where  $T$  is air temperature (K), and  $R_H$  is relative humidity (%).

To determine the accuracy of this method Gueymard<sup>27</sup> compared the predictions of Equation (1) with accurate measurements from various sources. Monthly average values of surface temperature, surface humidity, and radiosonde soundings were used. It was found that the predictions of Equation (1) were within the  $\pm 10\%$  scatter of the accurate measurements. For an instantaneous measurement, the prediction may be a little less accurate than for the monthly averages. As a conservative limit, Gueymard<sup>29</sup> uses an accuracy of  $\pm 20\%$  for the surface humidity method. This is accurate enough for the cell measurement technique developed in this work. When  $w < 0.5$  cm, the surface humidity method becomes less accurate, as low humidity is difficult to measure accurately and inversion layers sometimes form at low temperatures.

### Turbidity

Turbidity  $\beta$  characterises the scattering and absorption of light by small particles in the atmosphere, mostly dust, water, ice, or hygroscopic salt particles. Turbidity attenuates blue light more than red, hence making the spectrum redder. Turbidity is a difficult process to quantify as the particles can vary in size, in number, and in other subtle ways. However, it can be adequately described by an equation in two parameters,  $\alpha$  and  $\beta$ .<sup>30</sup> Parameter  $\beta$  is a measure of the 'amount' of turbidity, while  $\alpha$  characterises the particle size distribution (in other words, the 'type' of particles). High  $\beta$  corresponds to high turbidity, and high  $\alpha$  corresponds to small particles.

The value of  $\alpha$  varies relatively little. This allows a simplification of the model by specifying typical  $\alpha$  values for different environments, e.g., rural, urban or maritime. Turbidity is then reduced to a single parameter  $\beta$ . The lower the value of  $\alpha$  (bigger particles), the less spectrally selective the scattering is. In the extreme case of  $\alpha = 0$ , turbidity will cause broadband attenuation. This will not alter the shape of the solar spectrum, and so will not cause any spectral mismatch. Conversely, the higher the value of  $\alpha$  the larger the spectral mismatch error. For this work, since the objective was to determine worst-case limits on spectral mismatch error,  $\alpha$  was set to the highest value that occurs commonly—a rural aerosol. The SMARTS2 turbidity model used was the Shettle and Fenn rural aerosol.

The value of  $\beta$  varies between 0 and approximately 0.4. A subjective description<sup>31</sup> is : clean 0.0, clear 0.1, turbid 0.2, very turbid 0.4.  $\beta$  is highest in the tropics and in early summer. In the tropics, the annual mean value is  $\simeq 0.12$ . In temperate zones, the annual mean is  $\simeq 0.06$ .<sup>30</sup> Data for specific locations can be found in NREL's NSRDB/TMY dataset ([http://rredc.nrel.gov/solar/old\\_data/nsrdb/tmy2](http://rredc.nrel.gov/solar/old_data/nsrdb/tmy2)) or the NASA/Aeronet dataset (<http://aeronet.gsfc.nasa.gov:8080/>). There are many different measures of turbidity in use in addition to  $\beta$ , examples being  $\tau_{500}$  and BAOD. Conversions are described by Gueymard.<sup>29</sup>

This work requires only a rough estimate of turbidity. This can be obtained using a broadband irradiance measurement.<sup>29</sup> The only expensive instrument required is a pyrheliometer, which will, most likely, already be in use as the reference detector. (A pyrheliometer is a meteorological instrument that measures direct-beam irradiance. It consists of a detector that responds to the total power in sunlight of all wavelengths, housed in a collimating tube to restrict its field of view. Pyrheliometers are highly accurate and cost about US\$1500). Broadband irradiance is largely determined by three parameters—air-mass, turbidity, and water. Since air-mass and water can be easily measured, as described above, turbidity can be deduced simply from an irradiance measurement. In

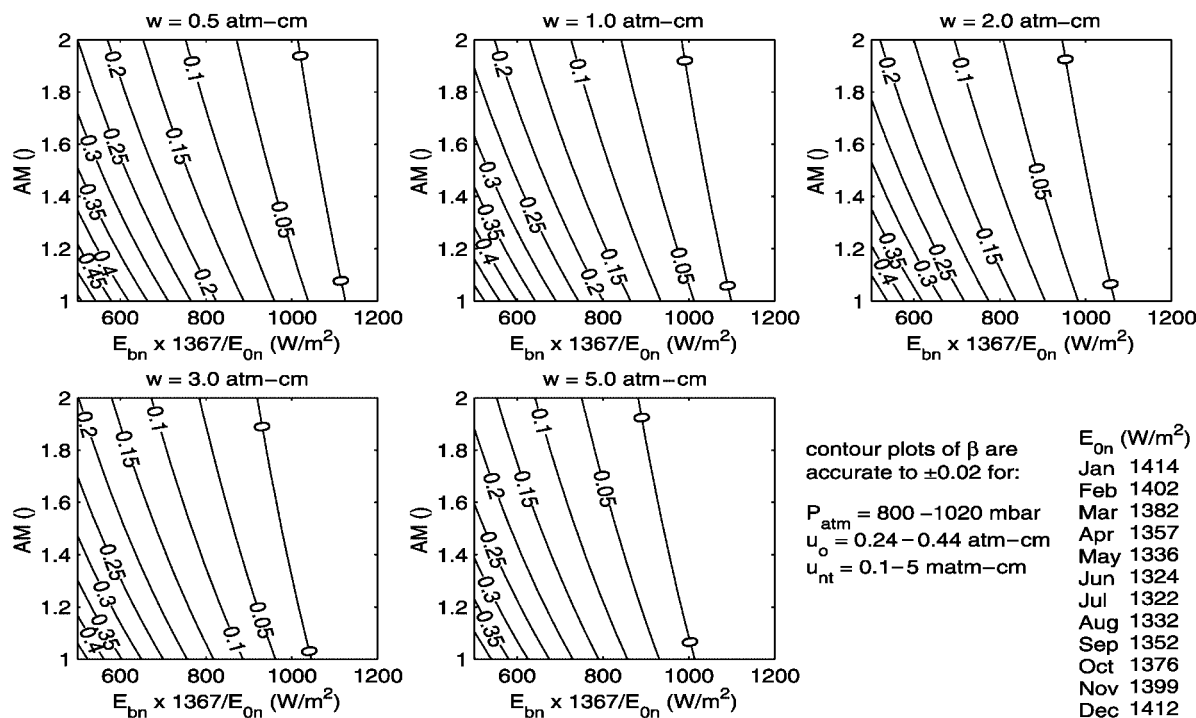


Figure 1. Contour plot of turbidity  $\beta$  as a function of precipitable water AM and direct beam irradiance

summary, turbidity can be determined as a function  $\beta(AM, p, E_{on}, w, E_{bn}, u_o, u_n)$ , where AM is airmass,  $p$  is atmospheric pressure,  $E_{on}$  is irradiance in space,  $w$  is precipitable water,  $E_{bn}$  is direct beam irradiance, and  $u_o$ ,  $u_n$  are amounts of ozone and  $\text{NO}_2$ . AM,  $p$ , and  $E_{on}$  can be calculated from time and location,  $w$  and  $E_{bn}$  can be measured, and  $u_o$  and  $u_n$  can be assumed ( $u_o = 0.34$  atm cm,  $u_n = 0.2$  matm cm). The equation to determine  $\beta$  is given in the paper by Gueymard.<sup>29</sup>

The equation to determine  $\beta$  is a function of seven variables so cannot be plotted. However, it can be reduced to a function of three variables, with only minor loss of accuracy, by making two simplifications. Firstly,  $E_{on}$  and  $E_{bn}$  can be combined into a single term since one is proportional to the other. The irradiance term in the simplified  $\beta$  function is the ratio:  $E_{bn} \times 1367/E_{on}$  ( $1367 \text{ W/m}^2$  is the mean value of  $E_{on}$ ). Values for  $E_{on}$  are tabulated in Figure 1. Secondly, the three parameters  $p$ ,  $u_o$  and  $u_n$  have a relatively minor effect on the turbidity estimation. Assumption of typical values for them results in a worst-case error in  $\beta$  of 0.02, which can be tolerated in this work. The simplified function is plotted in Figure 1. Use of the plot allows  $\beta$  to be estimated without typing in the lengthy code.

Gueymard tested the accuracy of turbidity determination from broadband irradiance by comparing the model predictions with accurate meteorological measurements under a wide range of conditions at several different locations. These showed that the method was accurate to  $\pm 0.02$  (absolute uncertainty,  $\beta$  is dimensionless). In the method proposed in this work, the meteorological measurements are less accurate, involving assumed values for ozone and  $\text{NO}_2$ , and measurement of  $w$  by the relative humidity method. Once these additional uncertainties are included, the broadband irradiance method is accurate to  $\pm 0.04$ . This is accurate enough for the cell measurement technique developed in this work.

There is an alternative broadband method for the measurement of turbidity, using the direct/diffuse ratio. It is insensitive to errors in precipitable water, ozone, and  $\text{NO}_2$ , but requires two instruments, a pyrheliometer for direct beam irradiance, and a shaded pyranometer for diffuse irradiance. It may also be less accurate for low turbidity, a condition of particular interest in this work. Consequently it was not used in this work.

## CELL MODELLING WITH PC1D

The spectral mismatch when measuring a cell is dependent on both the source spectrum and the characteristics of the cell. To investigate the effect of cell characteristics, a set of cells was simulated with the one-dimensional semiconductor-modelling package PC1D.<sup>32</sup> The cell set was chosen so as to encompass any likely crystalline-silicon solar cell.

Accurate measurement of a solar cell reduces to accurate measurement of  $I_{sc}$ , so in this work only  $I_{sc}$  was simulated. All of the major cell design parameters that influence  $I_{sc}$  were varied in the simulation. The design parameters, shown in Table II, determine the important generation and recombination processes within solar cells. Other parameters are of secondary importance. The values chosen for each of the parameters bracket the likely values to be found in a silicon solar cell. The simulations therefore treat all the worst-case possibilities. Two of the parameters require some explanation: first, the anti-reflection coatings were assumed to be optimal (i.e., maximising  $I_{sc}$  under AM1.5G). The modelling may not therefore represent coloured cells, such as are used for architectural applications, as they may have a strange spectral response. Secondly, doping levels (bulk and surface diffusions) were not varied. The effect of varying bulk doping is accommodated by varying the diffusion length, and the 'dead layer' effect of very high doping on the front surface is accommodated by the variation of front surface recombination. The range of front-surface recombination rates used here is intentionally quite extreme as the purpose of the simulations is to test the worst cases. Many common cells, such as screen-printed designs, will have intermediate values.

The optical model for textured cells in PC1D is approximate, so the simulated currents for textured cells will not be quite correct. However, since the modelling requires only a representative scatter of spectral response characteristics, this is not a serious limitation. Similarly, PC1D does not simulate three-dimensional effects, but these are usually small and not spectrally selective, so this is not a limitation for this work.

To give an indication of the range of cells simulated, the performance of the cell set is:  $I_{sc} = 15\text{--}43\text{ mA/cm}^2$ ,  $V_{oc} = 530\text{--}700\text{ mV}$ ,  $\eta = 6\text{--}25\%$ . The spectral responses of all cells in the cell set are shown in Figure 2.

The full cell set includes some very poor cells. To consider the more common situation of testing reasonable cells, a 'good' sub-set of the simulation results was also considered. Determining whether a cell is 'good' based on how it is constructed is difficult in practice—many parameters, such as recombination, are hard to measure. In contrast, it is easy to tell whether a cell is good from voltage and current density measurements—high voltage is an indication of low recombination, and high current is an indication of low recombination and good optical performance. As a rough guide, good-quality commercial cells under AM1.5G should have  $V_{oc} > 620\text{ mV}$  and  $J_{sc} > 35\text{ mA/cm}^2$  (for  $FF \approx 0.75$ ,  $\eta > 16\%$ ). The set of good cells was created by including only those cells that met these voltage and current density criteria. This subset included 177 of the original 864 cells.

Table II. Parameter values for the cells in the cell set; all 864 possible combinations were generated

| Cell parameter                       | Values  |
|--------------------------------------|---|
| Bulk lifetime ( $n, p$ )             | 0.1, 30, 10 000 $\mu\text{s}$   |
| Front-surface recombination          | $10^3, 10^7\text{ cm/s}$  |
| Rear-surface recombination           | $10^3, 10^7\text{ cm/s}$  |
| Thickness                            | 30, 100, 500 $\mu\text{m}$  |
| Front and rear internal reflectivity | 50, 100%  |
| Texturing                            | Textured, or polished   |
| Front-surface coating                | Bare silicon, bare silicon behind glass, SLAR, SLAR behind glass, DLAR, DLAR behind glass                                   |
| Cell base resistivity                | 1 $\Omega\text{ cm}$  |
| Diffusions ( $n^+/p/p^+$ )           | Gaussian profile, 0.8 $\mu\text{m}$ deep, maximum doping of $3 \times 10^{19}\text{ cm}^{-3}$ (100 $\Omega/\text{square}$ ) |
| Material properties                  | As for single-crystal silicon, at 25°C  |

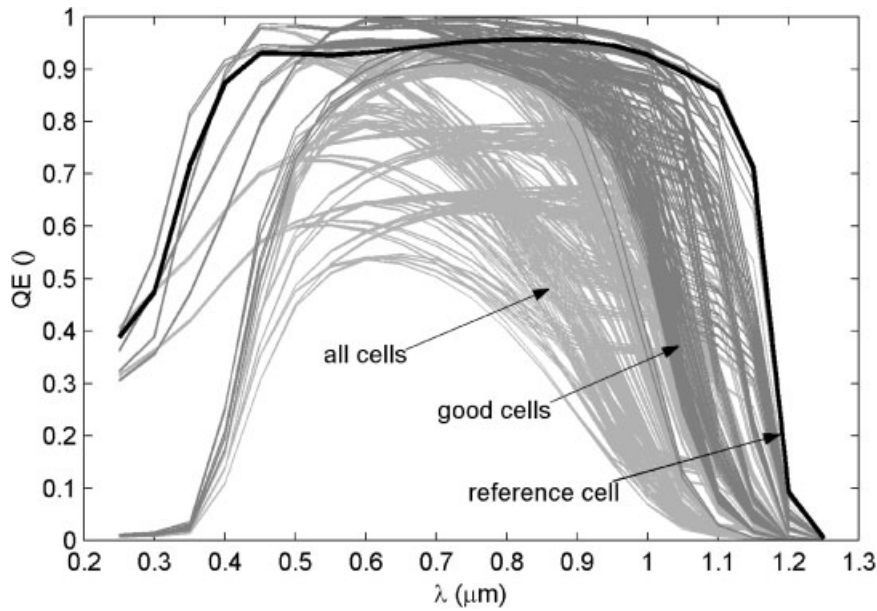


Figure 2. Spectral responses of all cells in the cell set

## CALCULATION OF SPECTRAL MISMATCH

After simulating the current for each of the 864 cells under each of the 1350 spectra and the two reference spectra (AM1.5D and AM1.5G), the spectral mismatch  $M$  was then calculated for the  $1.2 \times 10^6$  combinations:

$$M = \frac{I_{\text{sor}}/D_{\text{sor}}}{I_{\text{std}}/D_{\text{std}}} \quad (2)$$

where  $D$  is the output of the reference detector,  $I$  is the short-circuit current of the test cell, and subscripts sor and std refer to the source spectrum and standard spectrum, respectively.

The more common formulation for spectral mismatch, involving spectral responses and spectra, was not used, owing to uncertainty about how accurately PC1D calculates spectral responses. Instead, PC1D was used to directly calculate  $I_{\text{sc}}$  for each cell under each spectrum.

The spectral mismatch errors  $\varepsilon_M$ , were then calculated from the spectral mismatches:

$$\varepsilon_M = |1 - M| \quad (3)$$

Two reference detectors were considered in the modelling: a thermal detector, representing a pyrheliometer, and an excellent cell from the cell set, representing a calibrated silicon reference cell. For the thermal detector,  $D$  was the irradiance of the relevant spectrum, and for the reference cell,  $D$  was the cell current under the relevant spectrum.

The natural sunlight calibration method proposed in this work relies on the prediction of worst-case bounds on spectral mismatch error. It is therefore important to get an estimate of the uncertainty in the spectral mismatch figures. This uncertainty will be determined largely by the accuracy of the spectrum model, SMARTS2. The accuracy of PC1D is less important as it is being used only to generate a representative scatter of cell characteristics, not a prediction of the performance of a particular cell.

The accuracy of SMARTS2 is discussed in the documentation for the model.<sup>19</sup> It is stated that the model is accurate to approximately the measurement uncertainty of the commonly used LiCor LI-1800 spectroradiometer.



The uncertainty in  $M$  depends in a complicated way on both the uncertainty in the spectra and the uncertainty in the cells' spectral responses. The relationship has been extensively studied for its application to spectral mismatch correction. In one paper by Field,<sup>33</sup> which is particularly useful here, it was found that use of a LiCor LI-1800 to measure the spectrum resulted in the uncertainty in  $\varepsilon_M$  being  $\sim 5\%$  of  $\varepsilon_M$ . As the same type of spectroradiometer was used to verify SMARTS2, it can be concluded that the spectral mismatch error values calculated from SMARTS2 modelling should have an uncertainty of 5% (relative). The verification of SMARTS2, however, found that the errors from the model were only just within the uncertainty of the LI-1800, so the figure of 5% is probably a bit optimistic. For this work a more conservative value of 10% is used. To summarise, the uncertainty in  $\varepsilon_M$  is 10% relative (e.g., if  $M = 1.06$ , then  $\varepsilon_M = 0.06 \pm 0.006 = (6 \pm 0.6)\%$ ). In practice, the accuracy with which spectral mismatch error can be predicted will be limited more by measurements of atmospheric conditions than modelling accuracy, particularly given the simple techniques for atmospheric measurement proposed in this work.

## SIMULATION RESULTS

The results of the detailed simulations are shown in Figures 3–8. These are contour plots of the worst-case spectral mismatch error as a function of the three most important atmospheric parameters—air-mass, precipitable water, and turbidity. In these plots  $\text{NO}_2$  (0.1, 1, 5 atm cm) and altitude (0, 1, 2 km) vary in the background—at each point on the plots the largest (worst)  $\varepsilon_M$  was chosen out of all the  $\text{NO}_2$ , altitude, and cell possibilities.

Plots are shown for two standard spectra (AM1.5G and AM1.5D), two reference detectors (a pyrheliometer and a silicon cell), and for two cell sets (the full cell set, or the sub-set of good cells,  $V_{oc} > 620$  mV and  $J_{sc} > 35$  mA/cm<sup>2</sup>). For AM1.5D only the good cell set is shown, since AM1.5D is used for concentrator cells, which are usually of high performance.

## DISCUSSION

### *Lowest spectral mismatch error and best testing conditions*

The atmospheric conditions that give the lowest spectral mismatch error can be identified from the simulation results, Figures 3 to 8. The optimum conditions are a little different for AM1.5G and AM1.5D.

For AM1.5G (Figures 3–6), the optimum conditions are: air mass as low as possible ( $< 1.2$ ), turbidity as low as possible ( $< 0.05$ ), and precipitable water moderate (1–3 atm cm). These are typical summer conditions for an unpolluted location in temperate latitudes. Under these conditions, this work predicts a spectral mismatch error of less than 2%, so total measurement error of  $< 5\%$  should be achievable. This work has not yet been fully experimentally verified though, so it is premature to claim definitively that it is this good.

The effects of turbidity and precipitable water counteract each other, so if one is high the other needs to be high as well. Fortunately, nature provides this correlation—both turbidity and precipitable water are higher in summer and in locations closer to the equator.

Low levels of precipitable water ( $< 1$  atm cm) should be avoided. This will probably occur if the air temperature is  $< 10^\circ\text{C}$ , so high-altitude locations or winter testing may not be suitable. In any case, obtaining low air-mass in winter is not possible.

For AM1.5D, the optimum conditions are somewhat broader than for AM1.5G: air-mass around 1.4–1.6, turbidity around 0.1, and precipitable water around 1–2 atm cm. These conditions are very similar to the standard conditions used to generate the AM1.5D spectrum, as would be expected. The AM1.5D spectrum is currently being revised,<sup>22</sup> and the new spectrum will be for lower turbidity so the new AM1.5D spectrum will be more like the existing AM1.5G.

Spectral mismatch error changes gradually with atmospheric conditions, so the simple techniques for measuring precipitable water, turbidity, and air mass described earlier are accurate enough to distinguish good conditions from poor conditions.

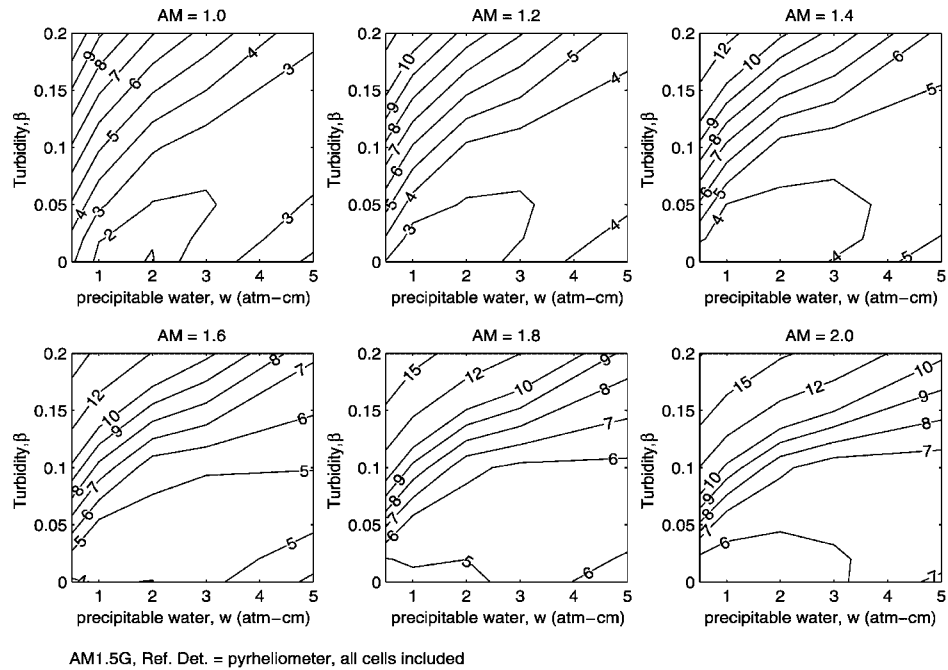


Figure 3. Worst-case  $\varepsilon_M$  (%). Standard spectrum AM1.5G; reference detector, pyrhelimeter; all cells included

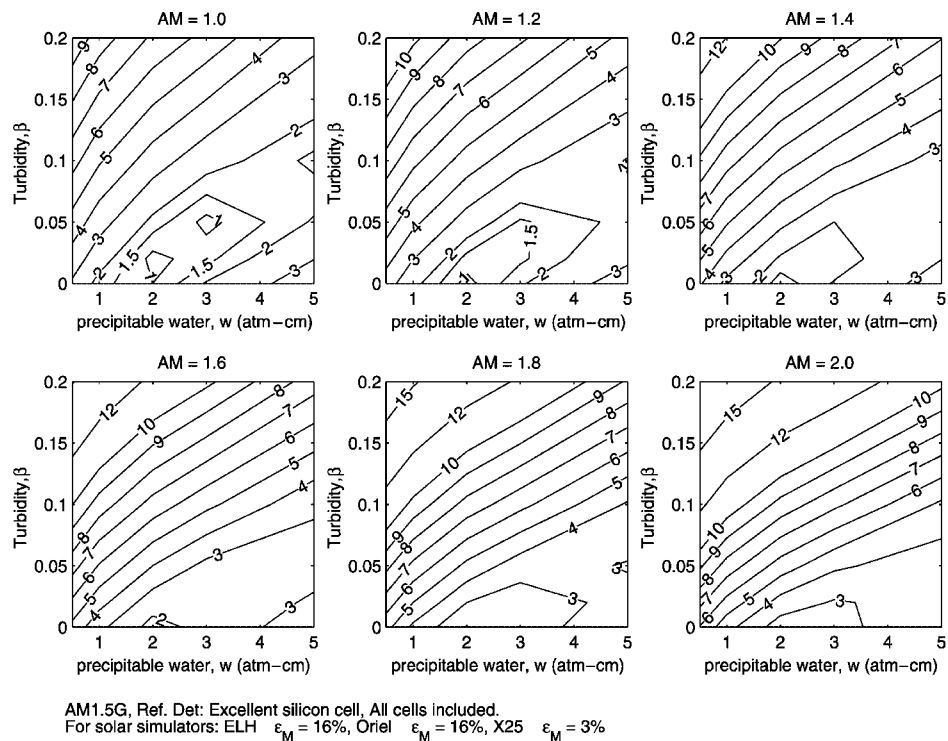


Figure 4. Worst-case  $\varepsilon_M$  (%). Standard spectrum AM1.5G; reference detector, excellent silicon cell; all cells included.  
Worst case figures for  $\varepsilon_M$  for solar simulators at bottom

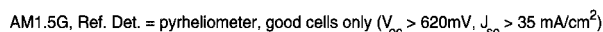


Figure 5. Worst-case  $\varepsilon_M(\%)$ . Standard spectrum AM1.5G; reference detector, pyrheliometer; only good cells included

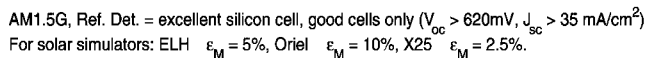


Figure 6. Worst-case  $\varepsilon_M(\%)$ . Standard spectrum AM1.5G; reference detector, excellent silicon cell; only good cells included. Worst case figures for  $\varepsilon_M$  for solar simulators at bottom

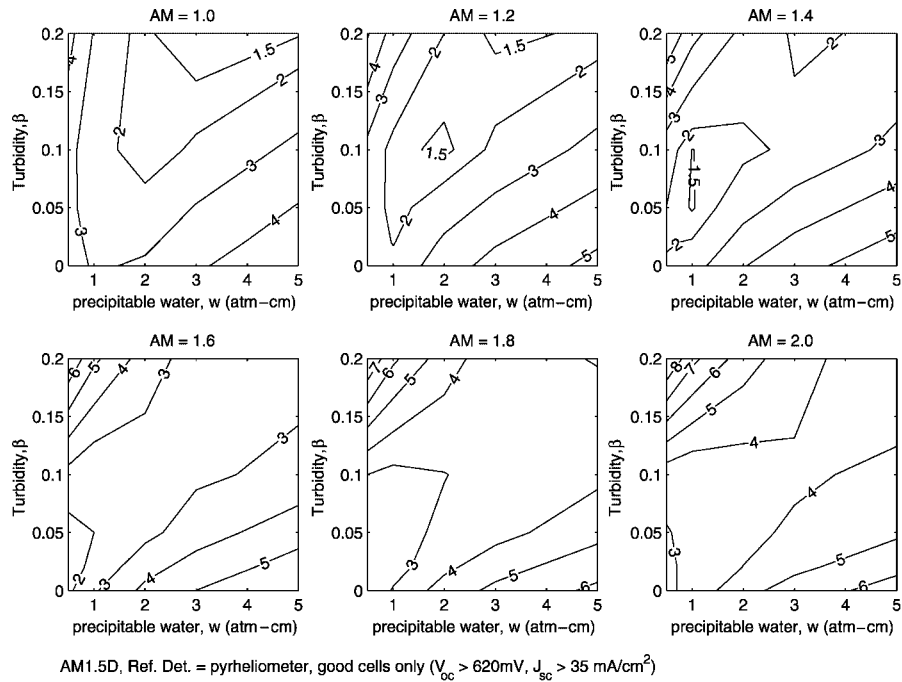


Figure 7. Worst-case  $\varepsilon_M(\%)$ . Standard spectrum AM1.5D; reference detector, pyrheliometer; only good cells included

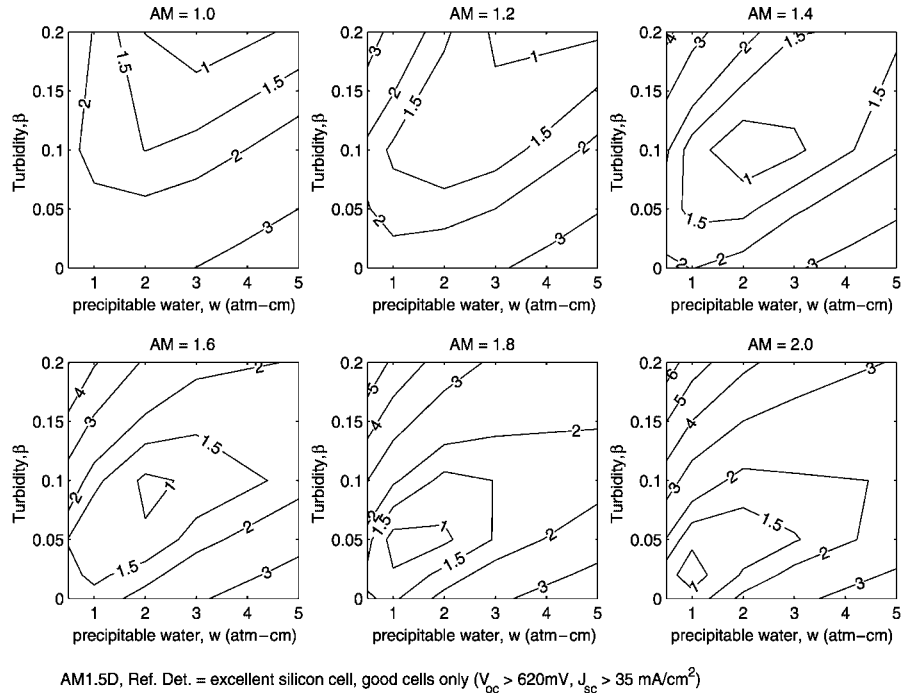


Figure 8. Worst-case  $\varepsilon_M(\%)$ . Standard spectrum AM1.5D; reference detector, excellent silicon cell; only good cells included

The contour plots show only a 'maximum' value of spectral mismatch error at each point. To test the robustness of the modelling the distributions of the spectral mismatch errors at several points in the contour plots of Figures 3 to 8 were examined (not shown in this paper owing to space limitations). The actual spectral mismatch distributions for the 864 cells are generally squarish, and do not have a long tail on either side. This gives confidence in the usefulness of the simulations, as it shows that all cells behave similarly and there are no disastrously bad cells. Consequently, it is unlikely that a real-world cell would give a spectral mismatch error much larger than any of the modelled cells.

### *Choice of reference detector*

Two types of reference detector were considered in the modelling—a pyrheliometer, and an excellent silicon cell. This section discusses which reference detector will give the most accurate measurements.

The uncertainty in a cell measurement under natural sunlight depends on the calibration uncertainty for the reference detector as well as the spectral mismatch error. The uncertainty in the calibration of a pyrheliometer is about 2%,<sup>10</sup> and the uncertainty for a silicon cell calibrated at a standards laboratory is in the range 2–5% (as discussed in the Introduction). Drift in reference detector calibration is an issue that should also be considered. Pyrheliometers are superior in this regard as they are commercial scientific instruments with well-known stability characteristics (guaranteed <1% drift per year).

The silicon detector gives lower spectral mismatch error under most atmospheric conditions, so if a cell can be obtained that is calibrated to 2% accuracy and is known to be stable, it will be the best choice of reference detector. If, on the other hand, the silicon cell calibration is only 5% accurate, then measurement with a pyrheliometer will be more accurate under almost all conditions (for the best testing conditions, the total uncertainty using a 2% accurate pyrheliometer is approximately half that for a 5% accurate silicon detector). At the current time, we recommend using a pyrheliometer as the reference detector.

This work led to the interesting observation that there are some silicon cells that are a better spectral response match to a thermal (flatband) detector than to a high-quality silicon cell. When considered in quantum efficiency terms, the spectral response of a high-quality silicon cell is close to unity between 0.3 and 1.1  $\mu\text{m}$ , and the spectral response of a flat-band detector is proportional to  $1/\lambda$ . A cell with QE that is high in the blue and gradually declines towards the IR (i.e., a cell that is thin and has poor light trapping, but excellent front-surface passivation) in fact has a spectral response somewhat like the thermal detector. We have examined numerically the case of a 30- $\mu\text{m}$ -thick cell with poor light trapping and front-surface recombination of  $10^3 \text{ cm/s}$ . We found that under the spectrum for a Spectrolab X-25 solar simulator the spectral mismatch with respect to a thermal detector is 0.6% compared with 1.1% for an excellent silicon reference cell. The consequence of this observation is that a thermal detector should not automatically be considered a poor choice of reference device when measuring silicon cells.

### *Effect of restricting the cell set*

It can be seen by comparing the results for all cells and good cells only (i.e., Figure 3 with Figure 5 and Figure 4 with Figure 6) that restricting the cell set to include only good cells ( $V_{\text{oc}} > 620 \text{ mV}$ ,  $J_{\text{sc}} > 35 \text{ mA/cm}^2$ ) decreases the mismatch error, and for both reference detectors. This is to be expected, since the cells in the good set are more similar to each other than the cells in the full set are, and also more similar to a thermal detector (the cells most different from a thermal detector are those with poor blue response and good IR response).

Restricting the cell set has a significant effect when spectral mismatch error is large; e.g., for  $\text{AM} = 2$ ,  $w = 1 \text{ cm}$ ,  $\beta = 0.1$ ,  $\varepsilon_M$  decreases from almost 10% to about 6%. So if measurements are being performed under poor conditions, considering a restricted cell set may give a useful improvement in accuracy (i.e., winter measurements may be possible for good cells). However, if conditions are good, using a restricted cell set gives little improvement in the spectral mismatch error.

Restricting the cell set is equivalent to making large changes to cell characteristics. Yet this results in relatively little change in the mismatch error. This suggests that the natural sunlight testing method is unlikely to be

caught out by an unusual cell, since the differences between any particular real world cell and one of the modelled cells should be smaller than the changes between good cells and poor cells.

### *Comparison with solar simulators*

The worst-case spectral mismatch under natural sunlight can be compared with the worst-case spectral mismatch under the three solar simulators, for AM1.5G and a silicon reference detector (see text at the bottom of Figures 4 and 6). Note that only spectral matching is being compared. Sunlight will have far better spatial uniformity than any simulator.

For the full cell set (Figure 4), ELH and Oriel are very similar at  $\varepsilon_M < 16\%$ . Natural sunlight measurement under any conditions should give a better result than using one of these simulators. The Spectrolab X-25 gives  $\varepsilon_M < 3\%$ . Natural sunlight measurement should equal or better this under good conditions, but could be significantly worse under bad conditions.

When the cell set is restricted to good cells (Figure 6): ELH  $\varepsilon_M < 5\%$ , Oriel  $\varepsilon_M < 10\%$ , X-25  $\varepsilon_M < 2.5\%$ . Natural sunlight measurements under good conditions will equal or better any of the simulators. Measurements under bad conditions will be significantly worse than ELH or X-25 simulators, but comparable to Oriel. This confirms that measurement under natural sunlight should be more accurate than under any low-cost simulator.

Interestingly, the simulation results show that the ELH lamp has a better spectrum than the Oriel simulator. This is a surprising result, as the graph of the Oriel spectrum looks much closer to AM1.5G than the graph of the ELH spectrum. Closer inspection however, shows that the Oriel spectrum has a bias towards the blue—that is, too much blue/UV, and insufficient IR—whereas the ELH spectrum is more balanced—insufficient UV and IR, balanced by excessive visible. The spectral responses of silicon solar cells vary mostly for blue and infrared wavelengths. Therefore the most poorly matched reference cell and test cell pair is one with good blue/poor red response and the other with good red/poor blue response. With such a cell pair under the skewed spectrum of the Oriel simulator the spectral mismatch from the blue region will add to the spectral mismatch from the IR region. Under the balanced ELH spectrum the spectral mismatch errors from the red and blue regions will tend to cancel. Consequently, the ELH spectrum can actually give less spectral mismatch. Of course, a single ELH lamp has much worse spatial light uniformity than an Oriel simulator, so for large-area cells the Oriel simulator would still be better, in spite of the poor spectrum.

This result will not apply to other cell technologies with different spectral responses. For example, amorphous silicon has its bandgap cut-off at around  $0.7\text{ }\mu\text{m}$  and so the ELH spectrum would be extremely skewed in this case.

The usual means of classifying the spectral quality of solar simulators is to measure the worst-case deviation from the standard spectrum (ASTM-E927). The result just discussed suggests that this classification may be misleading, and that the quality of the simulator can not be specified in isolation from the characteristics of the cells being tested.

### *How often can outdoor tests be done*

Outdoor testing can be done only when weather conditions are suitable. It is interesting to examine some climate data, for a variety of different locations, to estimate how often suitable conditions might be available. The technique will be most useful for sites within approximately  $45^\circ$  of the equator, where conditions close to AM1 will be available throughout summer, so the examination is limited to sites in this region. The only major PV manufacturing region that falls well outside  $45^\circ$  is Europe. Data was obtained for six locations: Canberra (Australia); Valencia (Spain), Boulder Colorado (USA), San Francisco, California (USA), Prescott, Arizona (USA), and North Bend, Oregon (USA). These locations cover a range of coastal and inland locations, both heavily and lightly urbanised. In some particularly cloudy parts of the world (e.g., northern Europe), clear days may be too rare for this technique to be useful. However, the sites discussed here are certainly not deserts. In particular, the Oregon coast is quite wet, yet it still has about five clear days per month in summer.

For measurement with respect to the AM1.5G standard spectrum: in summer, all locations have several days every month that are cloud free, all get close to  $AM=1$ , all have suitable levels of precipitable water

(1–3 atm cm), and most have suitable levels of turbidity ( $\beta < 0.1$ ), though in Valencia and San Francisco turbidity is typically 0.1–0.2, which is a bit high. Spectral mismatch error  $< 5\%$  should be achievable for several months of the year. In winter, air-mass is too high and precipitable water may be too low—spectral mismatch error could easily exceed 10%.

For measurement with respect to the AM1.5D standard spectrum, the weather constraints are far less severe. The number of clear days, air-mass, and turbidity should be suitable for all locations for most of the year. In winter, however, precipitable water may sometimes be too low. Spectral mismatch error  $< 5\%$  should be achievable in most locations and at most times of year.

The effect of cloud is worth considering as people may wish to make measurements when it is not perfectly clear. Theory predicts that light cloud does not strongly affect the spectrum, so should not have a dramatic effect on cell measurement. This prediction was confirmed during an experimental verification when a patch of clearly visible cirrus cloud drifted over the sun for half an hour, reducing the direct-beam irradiance by about 2%. The measurements of cell current divided by irradiance changed less than 1% during the cloudy period. This shows that accurate measurements can be made, even if the sky is not perfectly clear. Care should be taken to ensure that rapidly changing light levels do not introduce errors due to instrument time constants, particularly with slow-responding pyrheliometers.

### *Circumsolar radiation and design of collimating tube*

Measurement under direct-beam radiation requires a collimating tube to restrict the cell's field of view to direct-beam sunlight only. Circumsolar radiation, the diffuse light coming from the region of sky around the sun, can introduce errors if the reference device and the collimator housing the test cell see different angles of sky.

SMARTS2 includes circumsolar radiation in its direct beam spectrum, and can simulate a range of different collimator geometries. It was used in this work to determine how accurately the collimator geometry must match the reference device (assumed to be a pyrheliometer). Reference was also made to ASTM-E1125,<sup>7</sup> which describes a collimator design.

Circumsolar radiation is mainly due to aerosol scattering, and is strongest for large air-mass, high turbidity, large aerosol particle size, and high humidity.<sup>29</sup> A high-scattering atmosphere was therefore used in the modelling to determine an upper bound on the error due to circumsolar radiation ( $AM = 1.5$ , maritime aerosol,  $\beta = 0.2$ ,  $w = 5$  atm cm).

The geometry of a collimator is specified in terms of two half-angles, aperture angle  $\theta_a$ , and slope angle  $\theta_s$  (for a Kipp–Zonen CH1 pyrheliometer  $\theta_a = 2.5^\circ$  and  $\theta_s = 1^\circ$ ).

The modelling showed that if  $\theta_a = 2\text{--}3^\circ$  the measurement error due to circumsolar radiation will be  $< 1\%$ , which is acceptable. An additional requirement is that  $\theta_s$  should be  $> 1^\circ$  to allow for tracking inaccuracy and the finite angular size of the sun. In terms of linear dimensions for a cylindrical collimating tube of length  $L$ , internal radius  $R$ , and containing a cell of radius  $r$ , these angles correspond to:

$$L/R = 24 \pm 4 \quad \text{and} \quad R > 2r \quad (4)$$

This is the recommended geometry for the collimating tube. Note that the design requires only a minimum size for the tube diameter. This is convenient as it means that a collimator can be built to suit the largest cell likely to be tested, and the same collimator then used with smaller cells. It also means that the collimator can be a different shape from the cell (e.g., a circular collimating tube and a square cell).

It is important that the collimating tube has baffles and be blackened inside. This will prevent errors due to multiple reflections, either through capture of light from outside the nominal field of view, or through trapping of light reflected off the cell and surrounds.

### *Practical considerations*

It is easier to measure only  $I_{sc}$  outdoors.  $V_{oc}$  and FF can later be measured under a simulator adjusted according to the previously measured  $I_{sc}$  to give 1-sun current. This simplifies the jig required for outdoor measurements

by making temperature control and contacting arrangements less critical. It may also be more accurate, as it avoids the difficult problem of adjusting  $V_{oc}$  and FF from non-standard irradiance to 1-sun. However, higher accuracy is not certain since the simulator illumination will cause a slightly different generation profile in the cell. Some cells, particularly those with rear dielectric passivation and low base resistivity, are sensitive to changes in excess carrier concentration near the rear surface.

The  $I_{sc}$  values measured under natural sunlight will be obtained at non-standard illumination and will need to be corrected to 1-sun. This can be done by assuming linearity of  $I_{sc}$  with irradiance and scaling the measurement. Silicon cells are highly linear—even the worst cells have nonlinearities of only a few percent per decade change of light intensity.

An automatic sun-tracking platform, although convenient, is not essential. The sun moves at a leisurely  $0.25^\circ/\text{min}$ , allowing several minutes to align the equipment and take a measurement.

Temperature control of the cell is recommended, but not essential. The temperature sensitivity of  $I_{sc}$  for silicon cells is typically  $<0.1\%/^\circ\text{C}$ , so a temperature error of up to  $10^\circ\text{C}$  is tolerable. A cell with no heat-sinking can easily heat up by more than  $10^\circ\text{C}$  under 1-sun illumination, but one that is mounted on a large thermal mass and kept in the shade most of the time should be fine. In any case, a thermoelectrically cooled test block is easy to construct.

#### *Estimation of total measurement uncertainty*

The total measurement uncertainty for the technique proposed in this work can be estimated by summing all the component uncertainties. Note that this is a theoretical prediction of measurement uncertainty and so is probably optimistic. Experiments are required to verify these uncertainty estimates.

The major source of error comes from spectral mismatch, which according to the modelling can be 3–20%. The second largest error source is the calibration uncertainty for the reference detector, which for a pyrheliometer is 2%. There are also a range of minor error sources, each introducing  $<1\%$  uncertainty: circumsolar radiation; multiple reflections; temperature control;  $I_{sc}$  linearity; electrical instrument accuracy; tracking alignment; stray light; and time constants. The errors other than spectral mismatch total to 3.5% (root square sum). When added to a spectral mismatch error of at least 3%, the total uncertainty is no more than 2% greater than the spectral mismatch error.

In summary, the relative uncertainty in  $I_{sc}$  measurement is given, to a good approximation, by:

$$\Delta I_{sc}/I_{sc} = \varepsilon_M + 0.02$$

## **PRELIMINARY EXPERIMENTAL VERIFICATION**

To verify the predictions of this work, which are entirely theoretical and rely heavily on the accuracy of SMARTS2, a physical experiment was performed. Owing to time limitations, only a preliminary experiment was possible so the results are not conclusive. The verification experiment consisted of measuring a diverse set of cells under a range of atmospheric conditions, using the method described in this work. The relative change in the cell measurements over the range of atmospheric conditions was then compared with the relative change in the simulation results under the same conditions. For future, more thorough verification, it would be better to calibrate the cells by an external method (perhaps with the cooperation of some of the standards laboratories) and then compare with the measurements obtained with the natural sunlight method.

The cell set used for experimental verification was chosen to contain a diverse range of cell technologies. It included very-high-performance cells, commercial-quality screen-printed cells, low-quality lab prototype cells, and cells specially created to have extreme spectral responses. The cells were mounted on a temperature-controlled block and positioned behind a collimating tube designed according to the guidelines given earlier. Two reference devices were used: a Kipp & Zonen CH1 pyrheliometer and an excellent silicon cell mounted in its own collimating tube. Relative humidity and air temperature were measured with a Vaisala HM34 humidity and temperature meter. The equipment was aligned with the sun manually.



The cells were measured in three locations in southeastern Australia: Kioloa (coastal), Canberra (inland urban), and Mt Ginini (high altitude). The range of atmospheric conditions covered by the measurements did not encompass the full range used in the modelling, but was still reasonably wide. The conditions were: altitude 0–1.8 km; air-mass 1.4–2; precipitable water 0.5–2 cm; and turbidity 0.02–0.07.

The results for the pyrheliometer reference showed that the measured variations were slightly larger than the simulated variations ( $\pm 3\%$  compared with  $\pm 2\%$ ) if perfect measurement of turbidity and precipitable water was assumed. If the estimated uncertainty in turbidity and precipitable water was included, then the simulated variations were similar to the measured variations. Also, careful examination of the data suggests that there may have been problems with the data acquisition card measuring the pyrheliometer. For the silicon cell reference, the measured variations were always smaller than the simulated variations ( $< \pm 2\%$ ) over the full range of atmospheric conditions.

The results of the experimental verification are encouraging, but not conclusive as the measured variations were a little larger than the simulated variations. However, the variations were small (a few per cent) over a wide range of atmospheric conditions, which confirms that natural sunlight measurements are at least highly repeatable. To test the natural sunlight calibration method thoroughly a group of cells should be tested under a wider range of atmospheric conditions and some of them should be calibrated at a standards laboratory.

## CONCLUSIONS

The conclusion of this work is that calibration of solar cells under natural sunlight should be both convenient and accurate. A diagrammatic summary of the proposed method is shown in Figure 9. Modelling of a wide range of silicon solar cells under typical direct-beam solar spectra showed that:

- the spectrum of natural sunlight, under commonly occurring conditions, is a better match to the AM1.5G and AM1.5D standard spectra than a low-cost solar simulator and similar to an expensive simulator;

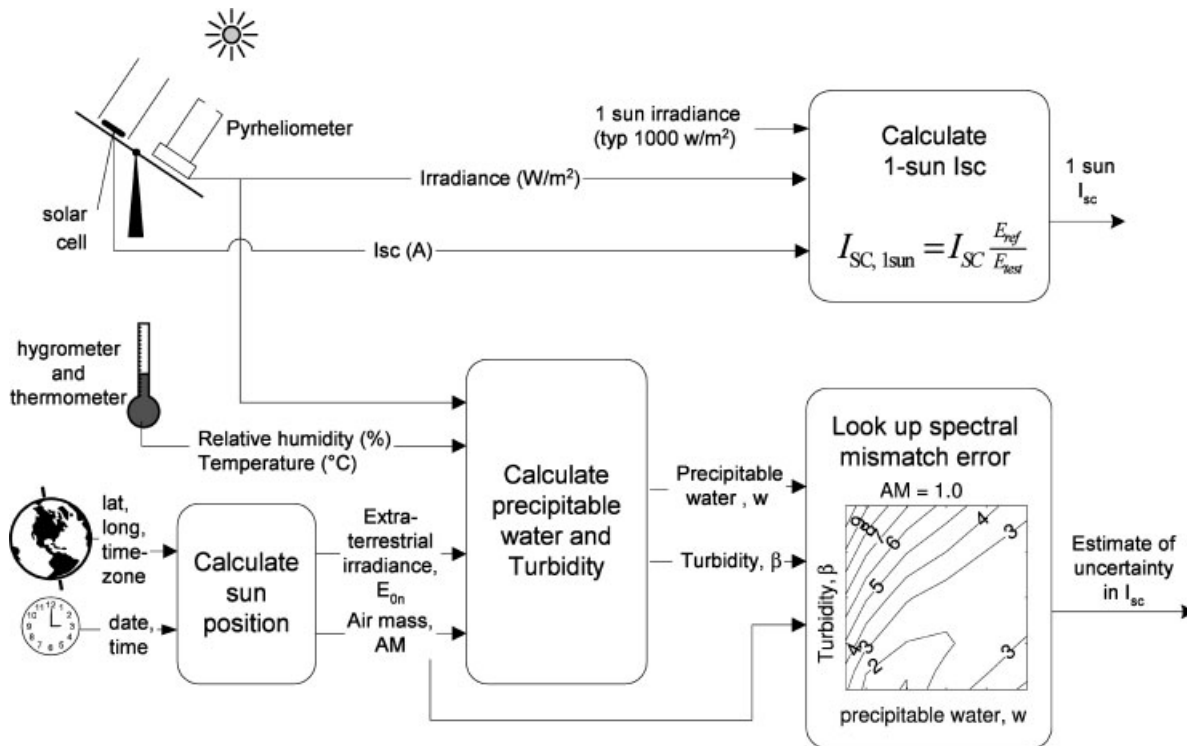


Figure 9. Diagrammatic summary of the proposed natural sunlight calibration method

- calibration under natural sunlight should be accurate—during summer, at most latitudes, a total measurement uncertainty below 5% should be achievable. Note: although this is close to the accuracy achieved by standards laboratories, this technique should not be considered a complete substitute for measurements at standards laboratories. There are many subtle ways errors can creep into measurements so it is essential to compare in-house measurements periodically with those from standards laboratories;
- calibration under natural sunlight is simple and little expensive equipment is required—the important atmospheric conditions can be estimated using only measurements of relative humidity, air temperature, direct-beam irradiance, time, and location;
- the technique is widely applicable—meteorological data for locations within 45° of the equator suggest that the required atmospheric conditions should occur commonly in summer.

A preliminary experiment to verify this method produced encouraging results, but was not conclusive. At the present time, the use of natural sunlight calibration seems inappropriately confined to high-accuracy calibrations performed only by standards laboratories. This work concludes that the method is far more widely applicable.

### Acknowledgements

We would like to thank Chris Gueymard for his many helpful e-mails about the spectrum model, SMARTS2, and Jeff Brown for building the collimating tube for outdoor experiments. The paper was improved by the detailed comments of four anonymous reviewers. The financial support of ERDC, in the form of a PhD scholarship, is gratefully acknowledged.

### REFERENCES

1. Seaman CH. Calibration of solar cells by the reference cell method—the spectral mismatch problem. *Solar Energy* 1982; **29**(4): 291–298.
2. Emery KA, Osterwald CR, Wells CV. Uncertainty analysis of photovoltaic efficiency measurements. *Proceedings of the 19th IEEE Photovoltaic Specialists Conference*, New Orleans, 1987; **1**: 153–159.
3. Berman D, Faiman D. EVA Browning and the time-dependence of *I*–*V* curve parameters on PV modules with and without mirror-enhancement in a desert environment. *Solar Energy Materials and Solar Cells* 1997; **45**(4): 401–412.
4. NASA CP-2010. *Terrestrial Photovoltaic Measurements II*. CP-2010, NASA, 1976.
5. NASA TM 73703. *Terrestrial Photovoltaic Measurement Procedures*. TM 73702, NASA, 1977.
6. Osterwald CR, Emery KA, Myers DR, Hart RE. Primary reference cell calibrations at SERI: history and methods. *Proceedings of the 21st IEEE Photovoltaic Specialists Conference*, Kissimmee, 1990; **2**: 1062–1067.
7. ASTM E1125. *ASTM E1125-99 Standard Test Method for Calibration of Primary Non-Concentrator Terrestrial Photovoltaic Reference Cells Using a Tabular Spectrum*. American Society for Testing and Materials, 100 Barr Harbor Drive, West Conshohocken, PA 19428-2959, USA, 1999.
8. Matson RJ, Emery KA, Bird RE. Terrestrial solar spectra, solar simulation and solar cell short-circuit current calibration: a review. *Solar Cells: Their Science, Technology, Applications and Economics* 1984; **11**(2): 105–145.
9. ASTM E1039. *ASTM E1039-99: Standard Test Method for Calibration of Silicon Non-Concentrator Photovoltaic Primary Reference Cells Under Global Irradiation*. American Society for Testing and Materials, 100 Barr Harbor Drive, West Conshohocken, PA 19428-2959, USA, 1999.
10. Myers DR. Estimates of uncertainty for measured spectra in the SERI spectral solar radiation database. *Solar Energy* 1989; **43**(6): 347–353.
11. Emery KA, Osterwald CR, Rummel S, Myers DR, Stoffel TL, Waddington D. A comparison of photovoltaic calibration methods. *Proceedings of the 9th E.C. Photovoltaic Solar Energy Conference*, Freiburg, 1989; 648–651.
12. Osterwald CR, Anevisky S, Barua AK, Dubard J, Emery K, King D, Metzendorf J, Nagamine F, Shimokawa R, Udayakumar N, Wang YX, Wittchen T, Zaaiman W, Zastrow A, Zhang J. Results of the PEP'93 intercomparison of reference cell calibrations and newer technology performance measurements. *Proceedings of the 25th IEEE Photovoltaic Specialists Conference*, Washington DC, 1996; 1263–1266.
13. Metzendorf J, Wittchen T, Heidler K, Dehne K, Shimokawa R, Nagamine F, Ossenbrink H, Fornarini L, Goodbody C, Davies M, Emery K, DeBlasio R. Objectives and results of the PEP'87 round-robin calibration of reference solar cells and modules. *Proceedings of the 21st IEEE Photovoltaic Specialists Conference*, Kissimmee, 1990; **2**: 952–959.

14. ASTM E1362. *ASTM E1362-99 Standard Test Method for Calibration of Non-Concentrator Photovoltaic Secondary Reference Cells*. American Society for Testing and Materials, 100 Barr Harbor Drive, West Conshohocken, PA 19428-2959, USA, 1999.
15. Green MA, Emery K. Solar cell efficiency tables: version 3. *Progress in Photovoltaics: Research and Applications* 1994; **2**: 27–34.
16. Mueller RL. The calculated influence of atmospheric conditions on solar cell  $I_{sc}$  under direct and global solar irradiances. *Proceedings of the 19th IEEE Photovoltaic Specialists Conference*, New Orleans, 1987: 166–170.
17. Osterwald CR. Calculated solar cell  $I_{sc}$  sensitivity to atmospheric conditions under direct and global irradiance. *Proceedings of the 18th IEEE Photovoltaic Specialists Conference*, Las Vegas, 1985: 951–956.
18. Keogh WM. Accurate performance measurement of silicon solar cells. *PhD Thesis*. Australian National University. 2001. [http://solar.anu.edu.au/pages/pdfs/2001\\_July\\_William\\_Keogh.pdf](http://solar.anu.edu.au/pages/pdfs/2001_July_William_Keogh.pdf) (accessed 19/8/03).
19. Gueymard C. *SMARTS2, a Simple Model of the Atmospheric Radiative Transfer of Sunshine*. FSEC-PF-270-95, Florida Solar Energy Centre, 1995.
20. Gueymard C. *SMARTS2 V2-8* 1996; <http://www.nrel.gov> (exact location unknown, 2003).
21. Air Force Research Lab. *MODTRAN* 2003; <http://www.vs.af.mil/Division/VSSSE/modtran4.html> (accessed 19/8/03).
22. Myers DR, Emery K, Gueymard C. Proposed reference spectral irradiance standards to improve concentrating photovoltaic system design and performance evaluation. *Proceedings of the 29th IEEE Photovoltaic Specialists Conference*, New Orleans, 2002; 923–926.
23. Emery K, Myers D, Rummel S. Solar simulation-problems and solutions. *Proceedings of the 20th IEEE Photovoltaic Specialists Conference*, Las Vegas, 1988; **2**: 1087–1091.
24. Oriel Corp. *Solar Simulation Catalog*. Oriel Corporation, 1993.
25. Bird R. *SPCTRAL2* 1986; <http://rredc.nrel.gov/solar/pubs/spectral/model> (accessed: Jan 2003)(NB: SPCTRAL2 was originally written in 1986, but the version on the NREL website is more recent).
26. Michalsky JJ. The Astronomical Almanac's algorithm for approximate solar position (1950–2050). *Solar Energy* 1988; **40**(3): 227–235.
27. Gueymard C. Assessment of the accuracy and computing speed of simplified saturation vapor equations using a new reference dataset. *Journal of Applied Meteorology* 1993; **32**(7): 1294–1300.
28. Gueymard C. Analysis of monthly average atmospheric precipitable water and turbidity in Canada and northern United States. *Solar Energy* 1994; **53**(1): 57–71.
29. Gueymard CA. Turbidity determination from broadband irradiance measurements—a detailed multicoefficient approach. *Journal of Applied Meteorology* 1998; **37**(4): 414–435.
30. Ångström A. Techniques of determining the turbidity of the atmosphere. *Tellus* 1961; **13**: 214–223.
31. Iqbal M. *An Introduction to Solar Radiation*. Academic Press Canada: Toronto, 1983.
32. Basore PA, Clugston DA. *PCID*. 5-3 1998; <http://www.pv.unsw.edu.au/pc1d> (accessed 17/2/2003).
33. Field H, Emery K. An uncertainty analysis of the spectral correction factor. *Proceedings of the 23rd IEEE Photovoltaic Specialists Conference*, Louisville, 1993; 1180–1187.